Research Article | Vol. 26, No. 4 | 19 Feb 2018 | OPTICS EXPRESS 3938
Optics EXPRESS

Characterizations of the nonlinear optical properties for (010) and ($\bar{2}$01) beta-phase gallium oxide

HONG CHEN, HOUQIANG FU, XUANQI HUANG, JOSSUE A. MONTES, TSUNG-HAN YANG, IZAK BARANOWSKI, AND YUJI ZHAO*

School of Electrical, Computer and Energy Engineering, Arizona State University, Tempe, AZ 85287, U.S.A.
**yuji.zhao@asu.edu*

Abstract: We report, for the first time, the characterizations on optical nonlinearities of beta-phase gallium oxide (β-Ga_2O_3), where both (010) β-Ga_2O_3 and ($\bar{2}$01) β-Ga_2O_3 were examined for two-photon absorption coefficient, Kerr nonlinear refractive index, and their polarization dependence. The wavelength dependence of two-photo absorption coefficient and Kerr nonlinear refractive index were also estimated by a widely used analytical model. β-Ga_2O_3 exhibits a two photon absorption (TPA) coefficient of 1.2 cm/GW for (010) β-Ga_2O_3 and 0.6 cm/GW for ($\bar{2}$01) β-Ga_2O_3. The Kerr nonlinear refractive index is -2.1×10^{-15} cm^2/W for (010) β-Ga_2O_3 and -2.9×10^{-15} cm^2/W for ($\bar{2}$01) β-Ga_2O_3. In addition, β-Ga_2O_3 shows stronger in-plane nonlinear optical anisotropy on ($\bar{2}$01) plane than on (010) plane. Compared with GaN, TPA coefficient of β-Ga_2O_3 is 20 times smaller, and the Kerr nonlinear refractive index of β-Ga_2O_3 is also found to be 4–5 times smaller. These results indicate that β-Ga_2O_3 have the potential for ultra-low loss waveguides and ultra-stable resonators and integrated photonics, especially in UV and visible wavelength spectral range.

OCIS codes: (160.4330) Nonlinear optical materials; (190.4180) Multiphoton processes; (160.1190) Anisotropic optical materials.

References and links

1. S. I. Stepanov, V. I. Nikolaev, V. E. Bougrov, and A. E. Romanov, "Gallium oxide: properties and applica a review," Rev. Adv. Mater. Sci. **44**, 63–86 (2016).
2. T. Oshima, K. Kaminaga, H. Mashiko, A. Mukai, K. Sasaki, T. Masui, A. Kuramata, S. Yamakoshi, and A. Ohtomo, "β-Ga2O3 single crystal as a photoelectrode for water splitting," Jpn. J. Appl. Phys. **52**(11R), 111102 (2013).
3. K. Sasaki, M. Higashiwaki, A. Kuramata, T. Masui, and S. Yamakoshi, "Ga2O3 Schottky Barrier Diodes Fabricated by Using Single-Crystal beta–Ga2O3 (010) Substrates," IEEE Electron Device Lett. **34**(4), 493–495 (2013).
4. H. Fu, H. Chen, X. Huang, I. Baranowski, J. Montes, T. H. Yang, and Y. Zhao, "Effect of crystalline anisotropy on vertical (–201) and (010) beta-Ga2O3 Schottky barrier diodes on EFG single-crystal substrates," arXiv preprint arXiv:1712.01318 (2017).
5. M. D. Sing, W. S. Liang, R. H. Horng, P. Ravadgar, T. Y. Wang, and H. Y. Lee, "Growth and characterization of Ga2O3 on sapphire substrates for UV sensor applications," Proc. SPIE **8263**, 826317 (2012).
6. Y. Zhao, S. Tanaka, C. C. Pan, K. Fujito, D. Feezell, J. S. Speck, S. P. DenBaars, and S. Nakamura, "High-power blue-violet semipolar (2021) InGaN/GaN light-emitting diodes with low efficiency droop at 200 A/cm2," Appl. Phys. Express **4**(8), 082104 (2011).
7. H. Fu, Z. Lu, X. H. Zhao, Y. H. Zhang, S. P. DenBaars, S. Nakamura, and Y. Zhao, "Study of Low-Efficiency Droop in Semipolar 20-2-1 InGaN Light-Emitting Diodes by Time-Resolved Photoluminescence," J. Disp. Technol. **12**(7), 736–741 (2016).
8. Y. Zhao, Q. Yan, C. Y. Huang, S. C. Huang, P. Shan Hsu, S. Tanaka, C. C. Pan, Y. Kawaguchi, K. Fujito, C. G. Van de Walle, J. S. Speck, S. P. DenBaars, S. Nakamura, and D. Feezell, "Indium incorporation and emission properties of nonpolar and semipolar InGaN quantum wells," Appl. Phys. Lett. **100**(20), 201108 (2012).
9. H. Fu, H. Chen, X. Huang, Z. Lu, and Y. Zhao, "Theoretical analysis of modulation doping effects on intersubband transition properties of semipolar AlGaN/GaN quantum well," J. Appl. Phys. **121**(1), 014501 (2017).

#315716 https://doi.org/10.1364/OE.26.003938
Journal © 2018 Received 14 Dec 2017; revised 27 Jan 2018; accepted 28 Jan 2018; published 6 Feb 2018

Optics EXPRESS

10. J. B. Limb, D. Yoo, J. H. Ryou, W. Lee, S. C. Shen, R. D. Dupuis, M. L. Reed, C. J. Collins, M. Wraback, D. Hanser, E. Preble, N. M. Williams, and K. Evans, "GaN ultraviolet avalanche photodiodes with optical gain greater than 1000 grown on GaN substrates by metal-organic chemical vapor deposition," Appl. Phys. Lett. **89**(1), 011112 (2006).
11. X. Huang, H. Fu, H. Chen, Z. Lu, I. Baranowski, J. Montes, T. H. Yang, B. P. Gunning, D. Koleske, and Y. Zhao, "Reliability analysis of InGaN/GaN multi-quantum-well solar cells under thermal stress," Appl. Phys. Lett. **111**(23), 233511 (2017).
12. X. Huang, H. Fu, H. Chen, X. Zhang, Z. Lu, J. Montes, M. Iza, S. P. DenBaars, S. Nakamura, and Y. Zhao, "Nonpolar and semipolar InGaN/GaN multiple-quantum-well solar cells with improved carrier collection efficiency," Appl. Phys. Lett. **110**(16), 161105 (2017).
13. C. Janowitz, V. Scherer, M. Mohamed, A. Krapf, H. Dwelk, R. Manzke, Z. Galazka, R. Uecker, K. Irmscher, R. Fornari, M. Michling, D. Schmeißer, J. R. Weber, J. B. Varley, and C. G. V. Walle, "Experimental electronic structure of In2O3 and Ga2O3," New J. Phys. **13**(8), 085014 (2011).
14. Z. Galazka, K. Irmscher, R. Uecker, R. Bertram, M. Pietsch, A. Kwasniewski, M. Naumann, T. Schulz, R. Schewski, D. Klimm, and M. Bickermann, "On the bulk β-Ga 2 O 3 single crystals grown by the Czochralski method," J. Cryst. Growth **404**, 184–191 (2014).
15. I. Bhaumik, R. Bhatt, S. Ganesamoorthy, A. Saxena, A. K. Karnal, P. K. Gupta, A. K. Sinha, and S. K. Deb, "Temperature-dependent index of refraction of monoclinic Ga2O3 single crystal," Appl. Opt. **50**(31), 6006–6010 (2011).
16. H. He, R. Orlando, M. A. Blanco, R. Pandey, E. Amzallag, I. Baraille, and M. Rérat, "First-principles study of the structural, electronic, and optical properties of Ga 2 O 3 in its monoclinic and hexagonal phases," Phys. Rev. B **74**(19), 195123 (2006).
17. Z. Guo, A. Verma, X. Wu, F. Sun, A. Hickman, T. Masui, A. Kuramata, M. Higashiwaki, D. Jena, and T. Luo, "Anisotropic thermal conductivity in single crystal β-gallium oxide," Appl. Phys. Lett. **106**(11), 111909 (2015).
18. H. Chen, H. Fu, X. Huang, X. Zhang, T. H. Yang, J. A. Montes, I. Baranowski, and Y. Zhao, "Low loss GaN waveguides at the visible spectral wavelengths for integrated photonics applications," Opt. Express **25**(25), 31758–31773 (2017).
19. H. Chen, X. Huang, H. Fu, Z. Lu, X. Zhang, J. A. Montes, and Y. Zhao, "Characterizations of nonlinear optical properties on GaN crystals in polar, nonpolar, and semipolar orientations," Appl. Phys. Lett. **110**(18), 181110 (2017).
20. A. Yariv, "Critical coupling and its control in optical waveguide-ring resonator systems," IEEE Photonics Technol. Lett. **14**(4), 483–485 (2002).
21. M. Sheik-Bahae, A. A. Said, T. H. Wei, D. J. Hagan, and E. W. Van Stryland, "Sensitive measurement of optical nonlinearities using a single beam," IEEE J. Quantum Electron. **26**(4), 760–769 (1990).
22. C. K. Sun, J. C. Liang, J. C. Wang, F. J. Kao, S. Keller, M. P. Mack, U. Mishra, and S. P. DenBaars, "Two-photon absorption study of GaN," Appl. Phys. Lett. **76**(4), 439–441 (2000).
23. L. Gallais and M. Commandré, "Laser-induced damage thresholds of bulk and coating optical materials at 1030 nm, 500 fs," Appl. Opt. **53**(4), A186–A196 (2014).
24. P. G. Eliseev, H. B. Sun, S. Juodkazis, T. Sugahara, S. Sakai, and H. Misawa, "Laser-induced damage threshold and surface processing of GaN at 400 nm wavelength," Jpn. J. Appl. Phys. **38**(7), 839 (1999).
25. M. Mero, J. Liu, W. Rudolph, D. Ristau, and K. Starke, "Scaling laws of femtosecond laser pulse induced breakdown in oxide films," Phys. Rev. B **71**(11), 115109 (2005).
26. S. Jena, R. B. Tokas, N. M. Kamble, S. Thakur, and N. K. Sahoo, "Optical properties and laser damage threshold of HfO2-SiO2 mixed composite thin films," Appl. Opt. **53**(5), 850–860 (2014).
27. Y. Fang, F. Zhou, J. Yang, X. Wu, Z. Xiao, Z. Li, and Y. Song, "Anisotropy of two-photon absorption and free-carrier effect in nonpolar GaN," Appl. Phys. Lett. **106**(13), 131903 (2015).
28. R. Desalvo, M. Sheik-Bahae, A. A. Said, D. J. Hagan, and E. W. Van Stryland, "Z-scan measurements of the anisotropy of nonlinear refraction and absorption in crystals," Opt. Lett. **18**(3), 194–196 (1993).
29. K. Wang, J. Zhou, L. Yuan, Y. Tao, J. Chen, P. Lu, and Z. L. Wang, "Anisotropic third-order optical nonlinearity of a single ZnO micro/nanowire," Nano Lett. **12**(2), 833–838 (2012).
30. V. Pačebutas, A. Krotkus, T. Suski, P. Perlin, and M. Leszczynski, "Photoconductive Z-scan measurement of multiphoton absorption in GaN," J. Appl. Phys. **92**(11), 6930–6932 (2002).
31. M. Sheik-Bahae, D. C. Hutchings, D. J. Hagan, and E. W. Van Stryland, "Dispersion of bound electron nonlinear refraction in solids," IEEE J. Quantum Electron. **27**(6), 1296–1309 (1991).
32. P. Zhang, X. Zhang, J. Xu, W. Mu, J. Xu, W. Li, and K. Chen, "Tunable nonlinear optical properties in nanocrystalline Si/SiO2 multilayers under femtosecond excitation," Nanoscale Res. Lett. **9**(1), 28 (2014).
33. R. W. Boyd, *Nonlinear Optics* (Academic, 2003).
34. Y. R. Shen, "The principles of nonlinear optics," New York Wiley-Interscience, (1984).
35. J. C. Phillips, "Dielectric definition of electronegativity," Phys. Rev. Lett. **20**(11), 550–553 (1968).
36. B. F. Levine, "Bond susceptibilities and ionicities in complex crystal structures," J. Chem. Phys. **59**(3), 1463–1486 (1973).
37. B. F. Levine, "Bond-charge calculation of nonlinear optical susceptibilities for various crystal structures," Phys. Rev. B **7**(6), 2600–2626 (1973).
38. K. Koynov, P. Mitev, I. Buchvarov, and S. Saltiel, "Calculation of third-order non-linear optical susceptibility of metal-oxide crystals," Pure Appl. Opt. Europ. Opt. Soc. P. A **5**(1), 89–93 (1996).

Optics EXPRESS

39. S. Geller, "Crystal Structure of β-Ga2O3," J. Chem. Phys. **33**(3), 676–684 (1960).

1. Introduction

As an emerging wide bandgap semiconductor material, beta-phase gallium oxide (β-Ga_2O_3) has attracted considerable attentions in catalysis [1,2], gas sensors [3], power electronics [4] and potential optical devices such as waveguides and resonators. Due to its wide bandgap (4.85 eV), β-Ga_2O_3 possesses a board transparent spectrum (>300 nm) from UV to visible wavelengths. Moreover, β-Ga_2O_3 is compatible with III-N material system [5]. This indicates β-Ga_2O_3 optical devices can integrate with III-nitride based visible light sources [6–8], detectors [9,10], and solar based applications [11,12]. Therefore, β-Ga_2O_3 is also a promising candidate for integrated photonics system, especially at UV and visible regime. In order to understand and improve the performances of various β-Ga_2O_3 devices, the comprehensive investigation on the material properties of β-Ga_2O_3 is of crucial importance. Intensive studies have been reported on the electronic [13], optical [14–16], and thermal properties [17] of β-Ga_2O_3. In terms of the optical properties of β-Ga_2O_3, previous researches mainly focused on the transmission [14], and refractive index [15,16]. However, the nonlinear optical properties of β-Ga_2O_3 have not been investigated yet, not to mention in UV and visible regime.

In UV and visible spectral range, under high optical power density, the performance of optical waveguides and resonators are mainly degraded by two-photon absorption (TPA) process [18,19]. For resonators that operate by critical coupling from bus waveguides, the refractive index shifting is governed by Kerr nonlinear refractive index at high power density and decreases the coupling efficiency especially in ultra-high quality factor resonators [20]. Therefore, in order to demonstrate high performance β-Ga_2O_3 based optical devices, it's critical to characterize the nonlinear optical properties of β-Ga_2O_3 including TPA coefficient and Kerr nonlinear refractive index.

To investigate and evaluate the nonlinear optical properties of β-Ga_2O_3 in visible spectral range, we performed a typical Z-scan characterization to study the TPA coefficient and Kerr nonlinear refractive index of β-Ga_2O_3. It's found that β-Ga_2O_3 has much smaller two photon absorption coefficient (20 times smaller) and Kerr nonlinear refractive index (4-5 times smaller) [18] than GaN, which is ideal for waveguides and resonators. Furthermore, due to the highly asymmetric crystalline structure of β-Ga_2O_3, the optical nonlinearity is also highly anisotropic. Relative higher in-plane nonlinear optical anisotropy was observed on $(\bar{2}01)$ plane than on (010) plane. These result can serve as references for the design of photonic devices based on β-Ga_2O_3.

This paper is organized as the following: In Section 2, we describe methods used in this work including experimental setup and theoretical models. In Section 3, we show our experimental results and make a discussion mainly on its significance in integrated photonics system. In section 4, we will draw the conclusion of this work.

2. Methods

The unintentionally doped (UID) β-Ga_2O_3 samples were provided by Tamura Corporation with a carrier concentration on the order of ~10^{17} cm^{-3} and a thickness of ~500 μm. The backside of the samples was polished by hand-grinding method with diamond lapping film of 0.5 μm grade. The polishing process was carefully controlled so that the thickness of the samples after polishing was reduced by less than 100 μm.

Figure 1(a) schematically shows the experimental setup of the Z-scan measurement [19–22] used in this study. Figure 1(b) depicts the crystal structure of β-Ga_2O_3, (010) and $(\bar{2}01)$ planes are also indicated. The light source was an ultrafast titanium-sapphire laser operating at 808 nm with 100 fs pulse width and 82 MHz repetition rate. A χ^2 crystal was used to generate second harmonic wave at the wavelength of 404 nm. The average power of input second harmonic beam was kept at 12 mW, which corresponds to ~7×10^9 W/cm^3 peak power density and ~0.7 mJ/cm^3 single pulse energy density. Due to the lack of reference, no

Optics EXPRESS

laser-induced damage threshold (LIDT) of β-Ga_2O_3 was found. As investigated in Ref [23], the LIDTs of dielectric materials are correlated to bandgap energy. To roughly estimate LIDT of β-Ga_2O_3, the LIDTs of two widely recorded materials, GaN (3.4 eV) and HfO_2 (5.2 eV), were checked. The threshold energy are ~5.4 J/cm^3 for GaN at 400 nm with 120 fs pulse width [24], and ranging from 0.5 J/cm^3 to 20 J/cm^3 for HfO_2 [25,26]. Those LIDTs are more than 500 times higher than the operation pulse energy density used in this work. Therefore, we neglected the laser-induced damage effects.

Half wavelength plate working on 404 nm was placed after χ^2 crystal for light polarization tuning. Beam was expanded by a set of lens before sending into optical objectives in order to fully utilize the numerical aperture. The samples were positioned between two optical objectives. An aperture was implemented in front of power meter to perform open and closed aperture testing.

To test the reliability of the setup, the beam size of the output light was used as an indicator. Based on Gaussian optics, with an incident beam diameter of 4 mm and a numerical aperture (NA) of 0.25, the calculated diameter of the output light is ~5 um (at 1/e^2) as shown in Fig. 1(c). This value is consistent with the beam diameter we extracted from open aperture Z-scan measurement in the next section.

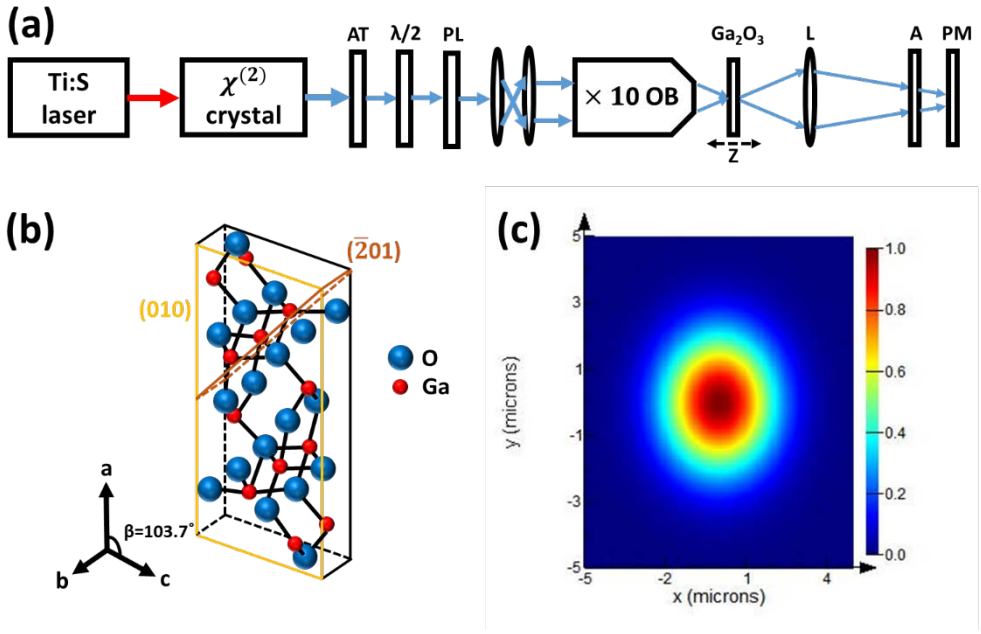

Fig. 1. (a) Experimental setup used in this work. AT indicates the attenuator, λ/2 the half-wavelength plate, PL the polarizer, OB the optical objective lens, A the aperture, PM the power meter. L1, L2, L3 are lenses. (b) Crystalline structure of β-Ga2O3 and planes that characterized in this study. (c) The field intensity at focal point estimated, which agree with our open aperture fitting.

The TPA coefficient and Kerr nonlinear refractive index can be obtained from open/closed aperture scanning based on Eqs. (1)–(3).

$$T \approx 1 - \frac{\alpha_{TPA} I_0 L_{eff}}{2\sqrt{2}} \times \frac{1}{1 + Z^2 / Z_0^2} \tag{1}$$

$$Z_0 = \frac{n\pi\omega_0^2}{\lambda} \tag{2}$$

Optics EXPRESS

$$n_{kerr} = \frac{\lambda \Delta \phi}{2\pi I_0 L_{eff}} \tag{3}$$

where T is the normalized transmission, I_0 is the peak beam power density, L_{eff} is the effective sample length, Z_0 is the Rayleigh range of the beam, n is the refractive index, ω_0 is the beam size at the focal plane, and λ is the wavelength in free space. L_{eff} is the sample thickness, $\Delta\phi$ the nonlinear phase shift due to Kerr effect [21], S parameter defined in [21] was controlled to be 0.35 throughout the characterization. More information about these equations can be found in Ref [18,20,21,26–29]. It's should be noted that the samples were tested at 404 nm which is above half bandgap energy of β-Ga_2O_3 (506 nm). Therefore, three-photon absorption modification to Eq. (1) is not necessarily needed [30]. The wavelength-dependence of the TPA coefficients was also theoretically calculated using Eq. (4),

$$\alpha_{TPA}(\omega) = K \frac{\sqrt{E_p}}{n_0^2 E_g^3} F_2(\hbar \cdot \omega / E_g) \tag{4}$$

where E_g is the direct bandgap energy and $E_p = 2|P_{vc}|^2 / m_0$, obtained by the $k \cdot p$ model [31], which is a material-independent parameter for direct bandgap semiconductors, n_0 is the refractive index, ω is the frequency, and K is a material-independent constant. F_2 is a fitting function with the form $F_2(x) = (2x-1)^{1.5} / (2x)^5$. In our theoretical analysis, we did not consider phonon assisted TPA because it only contributes to optical nonlinearity at a narrow bandwidth near 506 nm wavelength.

3. Experimental results and discussions

Figure 2 shows the open/closed aperture scanning results for (010) and ($\bar{2}$01) β-Ga_2O_3. Fitting the experimental data with Eqs. (1)–(3) yielded the TPA coefficients and Kerr nonlinear refractive index, which was summarized in Table 1. (010) β-Ga_2O_3 had a TPA coefficient α_{TPA} = 1.2 cm/GW and n_{kerr} = –2.1 × 10^{-15} cm^2/W when $\vec{E} \perp$ [102], while α_{TPA} of 0.6 cm/GW and n_{kerr} of –2.9 × 10^{-15} cm^2/W were obtained on ($\bar{2}$01) β-Ga_2O_3 when $\vec{E} \parallel$ [102]. The ($\bar{2}$01) β-Ga_2O_3 has smaller TPA coefficient than (010) β-Ga_2O_3. This result indicates ($\bar{2}$01) β-Ga_2O_3 waveguides and resonators will have less loss induced by TPA in visible spectral regime. On the other hand, ($\bar{2}$01) β-Ga_2O_3 has larger Kerr nonlinear refractive index. In addition, the output beam diameters were also obtained, which were in good agree with theoretical calculations based on Gaussian optics. It is worth noting that besides the transition from valance band (VB) to conduction band (CB), β-Ga_2O_3 exhibits up to three additional transition channels [1] that may contribute to the optical transition. Photon energies corresponding to the channels are: UV (3.2–3.6 eV), blue (2.8–3.0 eV), and green (2.4 eV). The green transition channel is mainly introduced by Be, Ge, and Sn dopants, therefore it is not a main factor in this work. The blue transition channel is originated from oxide vacancies and correlated to the n-type conductivity of sample. Those intermediate states may enhance the TPA process and introduce saturable one photon absorption [32]. But this process should have minimum effect in this study as the sample used in this work is UID bulk β-Ga_2O_3 with high crystalline quality. The UV transition channel is resulted from recombination between free electrons and self-trapped holes. The electrons deep inside VB are required to be excited in order to contribute to the absorption process, which is relatively less efficient than transition from VB to oxide vacancy states.

Optics EXPRESS

From Fig. 2, it can be clearly observed that closed aperture measurement exhibits more intense noise comparing with open aperture curve. This can be mainly attributed to two reasons: firstly, the testing wavelength was located at 404 nm which is the second harmonic beam from Ti:S laser. Therefore, comparing with our previous work [19], the laser power was ~80 times lower. It is the low power that makes the noise from beam nonidealities more significant, which results in the "bump" and "dip" features in Figs. 2(c) and 2(d) at Z~0.2 mm. Secondly, according to Ref [31], n_{kerr} is supposed to be zero near ~0.7E_g photon energy, which corresponds to 3.4 eV for β-Ga_2O_3. Since the testing photon energy at 404 nm is ~3.1 eV, the n_{kerr} is supposed to be in a relative small magnitude. This also increase testing difficulties throughout the experiment. To verify the closed aperture data, relation $Z_{pv} \approx 1.7Z_0$ was implemented [21], the Z_{pv} represents peak-valley distance in closed aperture scan and Z_0 was obtained from Eqs. (1) and (2). Fitting of Figs. 2(a) and 2(b) yielded Z_0 of 0.15 mm and 0.13 mm, corresponding to Z_{pv} of 0.25 mm and 0.22 mm, respectively. These are consistent with the measured (0.22 mm and 0.23 mm) Z_{pv} shown in Figs. 2(c) and 2(d).

It also worth noting that below 3.4 eV photon energy, using the widely implemented fitting model [31] developed by Sheik-Bahae *et al.* the n_{kerr} is supposed to be positive, while the n_{kerr} obtained in this work is negative. Such negative n_{kerr} value has profound physics behind. As suggested in [31], the n_{kerr} is contributed from TPA effect, Raman effect, linear stark effect, and quadratic stark effect. For n_{kerr} obtained at relative long wavelength, fitting model implementing only TPA effect is sufficient. However, at short wavelength (~0.7 E_g photon energy), contribution from TPA effect is approaching zero and quadratic stark effect contributes significant negative phase change which in turn gives n_{kerr}. This explains why negative n_{kerr} was obtained in this work.

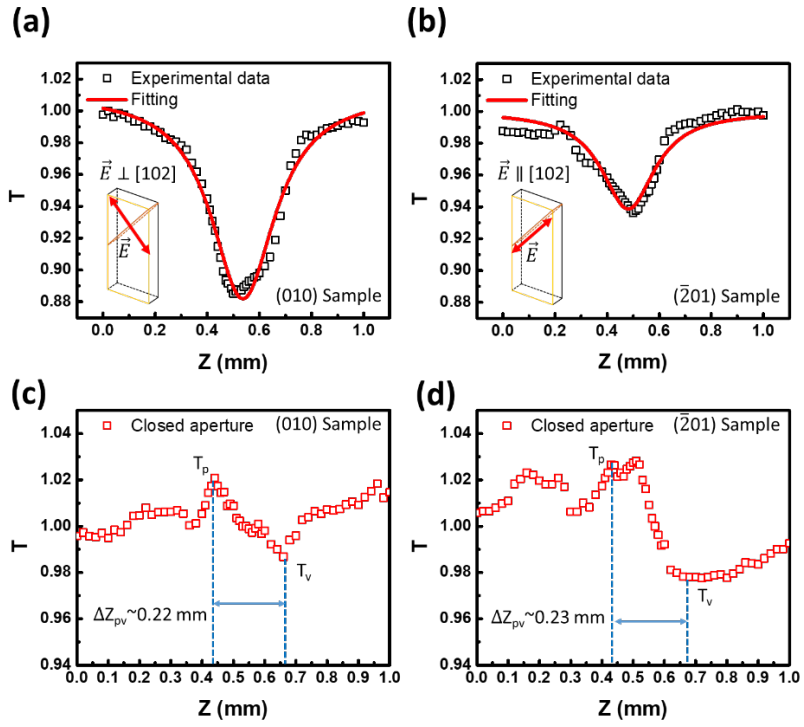

Fig. 2. Typical open aperture scanning curve obtained in this work. (a) Scan curve for (010) sample, (b) for ($\bar{2}$01) sample. (c) and (d), closed aperture Z-scan measurement of (010) and ($\bar{2}$01) samples, respectively.

Optics EXPRESS

Table 1. TPA coefficient, Kerr nonlinear refractive index obtained in this work for (010) and ($\bar{2}$01) samples. Beam diameter from fitting parameter is also shown.

(010), $\vec{E}$ ⊥ [102]			($\bar{2}$01), $\vec{E}$ ∥ [102]		
α_{TPA}(cm/GW)	n_{kerr}(cm^2/W)	R(μm)	α_{TPA}(cm/GW)	n_{kerr}(cm^2/W)	R(μm)
1.2	-2.1×10^{-15}	5.8	0.6	-2.9×10^{-15}	5.7

There are several physical models that can be implemented to understand the higher optical nonlinearity at (010) plane [33–38]. Quantum mechanical approach [33,34] calculates third order susceptibility accurately but requires intensive computing resources. Therefore it is only utilized in simple crystal structures [34]. A simplified bond-orbital model developed in [35–38] successfully explained the optical nonlinearities for various kind of materials including metal-oxide crystals [38]. We employed this model in this work to qualitatively understand the anisotropic nonlinearity of (010) and ($\bar{2}$01) β-Ga_2O_3. From bond orbital model, optical anisotropy of crystal is mainly contributed from bonding electrons between adjacent atoms [35]. While for other electrons that screening around individual atoms, the contribution to the optical anisotropy is less significant. As investigated comprehensively in [39], β-Ga_2O_3 is constructed by two types of gallium ions and three types of oxygen ions shown in Figs. 3(a) and 3(b). Type I gallium ion $Ga_{(I)}$ is surrounded by a distorted tetrahedron of oxygen ions with atom distance from 1.80 A to 1.85 A (1.83 A in average), type II gallium ion $Ga_{(II)}$ is surrounded by a distorted octahedron with atom distance from 1.95 A to 2.08 A (2.00 A in average). On (010) plane of β-Ga_2O_3, the bonds are not orderly orientated and therefore electrical field in (010) plane are more likely to interact with most of the bonds. However, on ($\bar{2}$01) plane, bonds between $Ga_{(I)}$ and $O_{(III)}$ are highly oriented along (010) direction. Such bonds have relative weak interaction with electric field polarized in ($\bar{2}$01) plane. The consequence is that the optical nonlinearity on ($\bar{2}$01) is relatively weaker than that on (010) plane.

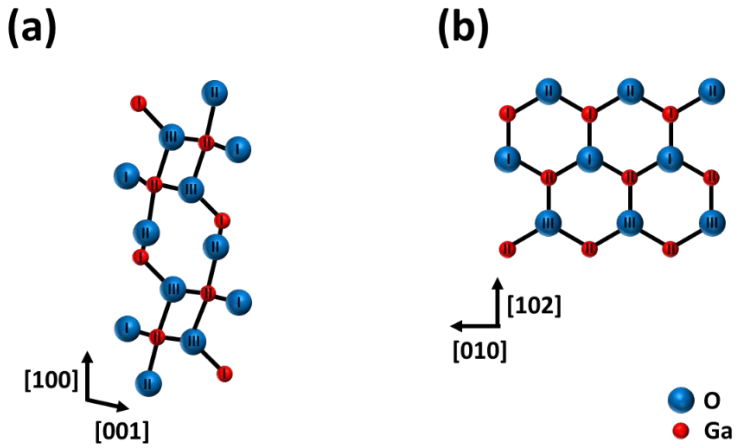

Fig. 3. Schematic view for the arrangement of ions inside β-Ga_2O_3, different types of ions are marked out by numbers. (a) Schematic view for (010) sample, (b) for ($\bar{2}$01) sample.

We previously estimated TPA coefficients and Kerr nonlinear refractive index for GaN [19] at same wavelength. The TPA coefficient of (010) and ($\bar{2}$01) β-Ga_2O_3 are ~10 and ~20 times smaller than that of GaN at 404 nm, respectively. Since the bandgap energy of β-Ga_2O_3

Optics EXPRESS

and GaN are different, we compare their nonlinear optical coefficient at same relative photon energy which is defined as E_p/E_g (0.63 for β-Ga_2O_3 tested at 404 nm). At E_p/E_g = 0.63 relative photon energy, TPA coefficient of (010) and ($\bar{2}$01) β-Ga_2O_3 samples are ~15 and ~30 times smaller than that of GaN. The high TPA coefficient observed in GaN might due to its exciton effects [22]. This result implies that β-Ga_2O_3 material is more capable to handle high optical power density applications in visible wavelength spectral range. Furthermore, Kerr nonlinear refractive index of β-Ga_2O_3 are also 4–5 times smaller at 404 nm and 5–7 times smaller at same relative photon energy than that of GaN. For optical applications that requires critical coupling, e.g. coupling from bus waveguide to ring or disk resonators, Kerr effect modifies the coupling efficiency at high optical power density, especially in those high resonance quality factor resonators [20]. Therefore, β-Ga_2O_3 based resonators will exhibit extreme coupling stability under high power operation comparing with GaN based resonators.

Figure 4 represents the polarization dependences of transmission minimum of (010) and ($\bar{2}$01) β-Ga_2O_3 during open aperture testing. Since β-Ga_2O_3 has a monoclinic crystal structure (Fig. 1), 41 independent nonzero elements are required to fully describe its third order nonlinearity d_{il}. Therefore, it is very difficult and inconvenient to find explicit expression for d_{eff} using polarization angle and individual nonlinear component d_{il} [21,22,27,28]. To describe the in-plane anisotropic nonlinearity clearly, we use $\Delta T_{max}/\Delta T_{min}$ in this work. Relative higher in-plane nonlinear optical anisotropy was found on ($\bar{2}$01) β-Ga_2O_3 with $\Delta T_{max}/\Delta T_{min}$ of 1.93 while (010) β-Ga_2O_3 had a $\Delta T_{max}/\Delta T_{min}$ of 1.29.

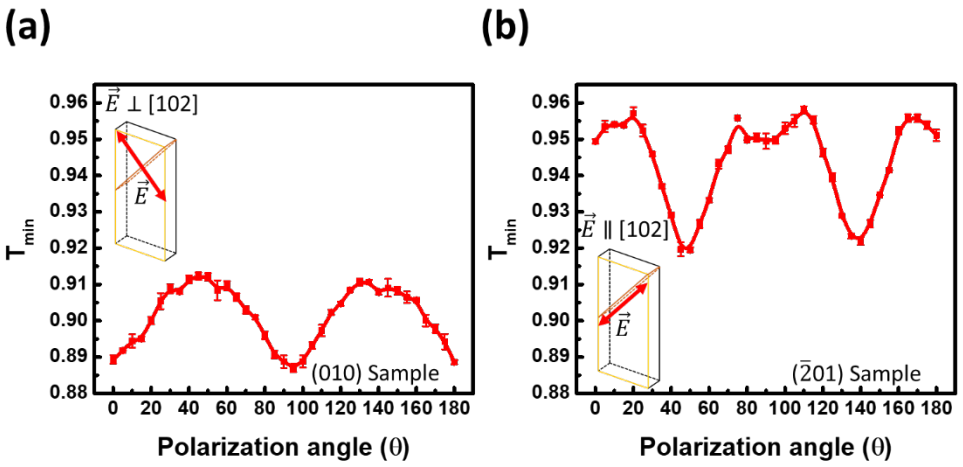

Fig. 4. Polarization dependence of minimum transmittance obtained in this work. (a) Polarization dependence for (010) sample, (b) for ($\bar{2}$01) sample.

Figure 5 shows the wavelength dependence of TPA coefficient using Eq. (4) for (010) and ($\bar{2}$01) β-Ga_2O_3. For (010) β-Ga_2O_3, $E\perp$ has larger TPA coefficient that $E\parallel$. For ($\bar{2}$01) β-Ga_2O_3, $E\perp$ has smaller TPA coefficient that $E\parallel$. Highest TPA absorption coefficient is observed in (010) β-Ga_2O_3 when electric field is perpendicular to [102] direction, while lowest TPA coefficient is obtained on ($\bar{2}$01) β-Ga_2O_3 when electric field is parallel to [102] direction. For each plane, the polarization dependence of TPA coefficient is a function of multiple physical parameters [38] such as bond iconicity, covalent radii, etc. It is extremely difficult to give a quantitative explanation and out of the scope of this work. Future experimental and theoretical studies are undergoing to clarify its polarization dependence. For both samples, the maximum TPA absorption occurs at ~360 nm wavelength. For wavelength above 360 nm, TPA coefficient decreases as wavelength increases. It can be attributed to the decreased excitation energy with increasing wavelength. While for wavelength below 360

Optics EXPRESS

nm, the TPA coefficient increase with increasing wavelength as the transition approaches its resonance wavelength.

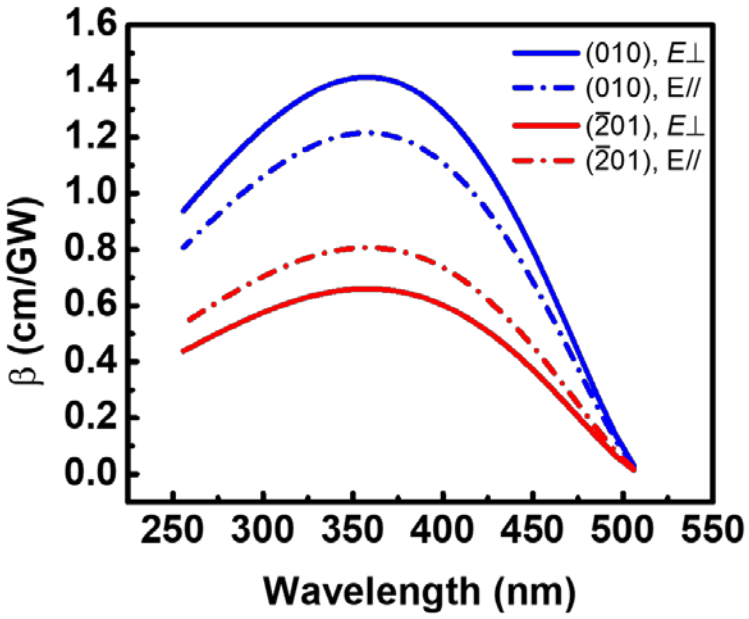

Fig. 5. The estimated wavelength dependence of TPA coefficient for (010) and ($\bar{2}$01) samples. "$E\perp$" indicates that the electrical field intensity is perpendicular to [102] direction, while "$E\|\|$" indicates that field intensity is parallel to [102] direction

4. Conclusions

We characterized the TPA coefficient and Kerr nonlinear refractive index of both (010) and ($\bar{2}$01) β-Ga_2O_3. TPA coefficient of Ga_2O_3 was found to be 10 to 20 times smaller than that of GaN at 404 nm. The Kerr nonlinear refractive index of Ga_2O_3 was 4 to 5 times lower than that of GaN. Therefore, due to its ultra-low TPA coefficient and its small Kerr nonlinear refractive index, β-Ga_2O_3 has the potential to serve as a more efficient platform for integrated photonic applications in UV and visible spectral range. Furthermore, the optical nonlinearities of β-Ga_2O_3 is highly anisotropic due to the asymmetric crystal structure of β-Ga_2O_3. These results can serve as guidelines for designing β-Ga_2O_3 based integrated photonics system.

5. Acknowledgement

The authors thank Dr. Michael Gerhold of US Army Research Office for the helpful discussion. This work is supported by the Bisgrove Scholar Program from Science Foundation Arizona. We gratefully acknowledge the use of facilities within the LeRoy Eyring Center for Solid State Science and CLAS Ultra Fast Laser Facility at Arizona State University.